Development and Characterization of Novel Nanoparticulate Gel Formulation for The State-of-the-Art Treatment in Topical Infection

[1]Mohammad Mujahid, [2]Md Arif Naseer, [3]Nasiruddin Ahmad Farooqui ,

[1]Department of Pharmaceutical Sciences, Adarsh Vijendra Institute of Pharmaceutical Sciences, Shobhit University, Saharanpur, Uttar Pradesh, India
[2]Department of Pharmaceutical chemistry, School of Pharmacy and Paramedical Sciences, K.K. University, Nalanda, Bihar, India
[3]Department of Pharmacy, Translam Institute of Pharmaceutical Education and Research, Meerut, Uttar Pradesh, India
Corresponding Author:
***Corresponding Author:** Mohammad Mujahid, Department of Pharmaceutical Sciences, Adarsh Vijendra Institute of Pharmaceutical Sciences, Shobhit University, Saharanpur, Uttar Pradesh, India*

KEYWORDS

Mometasone Furoate; Phospholipid;Nanoparticulate gel; Stability; Psoriasis.

ABSTRACT

Mometasone is indicated in psoriasis and dermatitis, has poorwater solubility and low bioavailability causes skin irritation andhair follicle inflammation. To achieve a protective base for mometasone topically, an MF-PL complex-embedded NP-loaded gel was developed. MF-PL complex was prepared using the thin-film hydration method and was characterized for percentage yield,percentage drug complexation, and drug loading. Nanoparticles were incorporated into the gel base and subjected to yield, mometasone release, solution homogeneity, and particle size assessments.The objectives were to improve the drug release profile, loading capacity, permeation, and patient compliance, and to conduct stability studies. The crystalline form of mometasone furoate, melting point (219±1.0 to 225±1.0°C), and partition coefficient (4.19±0.385) confirmed its purity and lipophilic nature. DSC, UV-visible spectrophotometry, and FTIR analyses confirmed the purity and compatibility of the drug and excipients.The nanoparticle formulations exhibited homogeneous dispersion and physical stability, with formulation F.7A4 demonstrating excellent stability (zeta potential: -37.5 mV, hydrodynamic diameter: 191.60 nm). TEM and SEM confirmed the uniform shape, smooth surface texture, and nanometre-sized particles. The optimized MF-loaded phospholipid nanoparticle gel (F.7A4 (G-2)) exhibited a suitable pH (6.24±0.031), viscosity (2444±2.08 cps), high spreadability (7.23±0.021 g.cm/sec), and drug content (98.535%).Thestudy concluded that the MF-PL nanoparticle gel was successfully formulated and can be employed in the treatment of psoriasis and skin dermatitis with minimal side effects.

1. Introduction

Mometasone furoate is a corticosteroid commonly used in the treatment of skin diseases, but its efficacy can be limited by its poor bioavailability and potential side effects(Taléns-Visconti et al., 2022). Skin diseases are a major health concern worldwide, affecting millions of people and causing significant morbidity and mortality(Basra & Shahrukh, 2009). Previous studies have shown that mometasone furoate can be effective in the treatment of skin diseases, but its use is often limited by its poor bioavailability and potential side effects(Taléns-Visconti et al., 2022). Despite the known efficacy of mometasone furoate in the treatment of skin diseases, there is a lack of research on its use in the form of phospholipid nanoparticle gel, which may improve its bioavailability and reduce side effects(Karole et al., 2022). The development of a more effective and safe treatment for skin diseases is crucial for improving patient outcomes and quality of life.

Mometasone, a drug used to treat asthma, inhibits the activity of mast cells, eosinophils, basophils, and lymphocytes (Marone, 1995). In addition, it suppresses the production of leukotrienes, histamine, and cytokines. When taken, corticosteroids, such as mometasone, diffuse through the cell membrane and reach the cytosol of cells, where they bind to glucocorticoid receptors (GR) to exert their therapeutic effects (Branco et al., 2018). MF has a 22-fold higher receptor affinity for GR than DS (dexamethasone), which results in a conformational change in the receptor, dissociation from the chaperone, and translocation of the receptor into the nucleus. Once inside the nucleus, receptors bind to glucocorticoid response elements (GREs), which either increase or decrease the production of anti-inflammatory molecules. This action also prevents transcription factors, including nuclear factor kappa B (NF-kappa B) and activator protein-1, by blocking inflammation (Lee &Burckart, 1998).

Pharmaceutical gel is one of the most commonly used DDS due to its versatility and compatibility with various drug substances. They are highly effective for multiple routes of administration, making them an excellent choice for delivering medications(Archana et al., 2022). Penetration-enhancing gels, in particular, are preferred for the administration of anti-inflammatory and anti-nausea drugs. These gels are relatively simple to prepare and provide significant efficacy.The USP/NF describe gels or jellies as semi-solid systems that consist of suspensions containing either tiny inorganic particles or bigger organic molecules interwoven in a liquid(Xu et al., 2020).

Nanoparticulate gel formulations are a popular type of nanotechnology-based delivery system. The formulations combine nanoparticles with gel matrices to create a hybrid system that leverages the advantages of both components. The gel matrix provides a good surface for sustained and controlled release, while nanoparticles help deliver the target and enhance penetration through the skin barrier (Patravale et al., 2008). Nanoparticle gel formulations are particularly beneficial in the treatment of dermatological diseases because they can provide prolonged and regulated drug release, improve drug stability, and enhance drug penetration into the skin (Ho Lee, 2014).

2. Materials and Methods

2.1Materials

Authentic mometasone furoate as agift sample was obtained from Neuland Laboratories (Hyderabad, India). Phospholipids were purchased from Lipoid GmbH (Germany), whereas Carbopol 934P grade was procured from Maruti Chemicals, Ahmedabad (Gujarat), India. Methanol, ethanol, chloroform, dichloromethane (DCM), and acetone were obtained from F.S. India Pvt. Ltd., Mumbai, India. Potassium dihydrogen orthophosphate and disodium hydrogen orthophosphate were procured from Thomas Baker (Chemicals) Pvt. Ltd. (Mumbai, India). For this study, 24 male Wistar rats (8–9 weeks of age, weighing 140–200 g) were used. The rats were procured from the Committee for the Purpose of Control and Supervision of Experiments on Animals (CCSEA) and the study was approved by the Institutional Animal Ethics Committee (IAEC/PH-23/TIPER/193 01/06/23).

2.2 Methods

2.2.1Pre-formulation studies

2.2.1.1 Organoleptic properties

A small amount of mometasone furoate was placed on white paper to observe its form, and the sample was visually examined under natural daylight against a white background to determine its colour. A minimal quantity of the drug sample of MF was taken in a glass vial and gently shaken. The vial was then uncapped and the odour was assessed.Taste assessment was not conducted because of the safety protocols.

2.2.1.2 Melting point

The MP of the MF was measured by using the USP technique. Initially, a little quantity of mometasone furoate was finely powdered and packed into a capillary tube by gently tapping it until the powder settled to a height of approximately 2-3 mm at the bottom. The capillary tube with drug sample was then kept in the MP apparatus. The temp. of the apparatus was incrementally raised in a controlled rate of 1-2°C per minute to accurately measure the drug's melting point.

2.2.1.3 Solubility

An excess amount of mometasone furoate (50 mg) was weighed and added to 10 ml of each solvent (methanol, ethanol, DCM, Distilled water, and phosphate buffer) in separate centrifuge tubes. The tubes were vortexed for 5 min to thoroughly mix the contents. Incubated these tubes at 25°C for 24 hours with intermittent shaking to ensure equilibrium. The samples were then centrifuged at 15,000 rpm for 15 min. to isolate the non-soluble drug from the clear liquid. The clear liquid was carefully collected and filtered through a 0.45 µm membrane filter to separate any remaining insoluble particles. This filtered clear liquid was analyzed using UV-Vis spectroscopy to determine the concentration of dissolved mometasone furoate.

2.2.1.4 Partition coefficient

A small amount of MF (approximately 10 mg) was accurately weighed and solubilized it in 10.0 mL of n-octanol saturated with water. This solution was combined with an equal volume (10.0 ml) of n-octanol-saturated water in a separatory funnel. The separatory funnel was shaken vigorously for 30 min to ensure thorough mixing and to allow the phases to separate completely for at least 1 h at room temperature.The aqueous and octanol layers were then carefully separated. The samples were spun at 15,000 rpm for 15 min to obtain clear phase separation. The separated aqueous and octanol layers were strained using a 0.45 µm membrane filter to isolate insoluble particles.The concentrations of mometasone furoate in both the octanol and aqueous phases were measured using a UV spectrophotometer at a wavelength of 248 nm.

2.2.2DSC Analysis of Drug (MF), Excipient (PL) and its Physical Mixture

Mometasone furoate or phospholipid (1–5 mg) was weighed separately and then placed in separate aluminum DSC pans. The pan was sealed with a lid to prevent sample loss during heating. The prepared sample pan was loaded into the temperature-controlled DSC instrument (Modal DSC 8000,PerkinElmer, New Delhi, India) along with a blank reference pan. DSC was run at a controlled heating rate (10°C/min) from ambient temperature to temperature above the expected MP of mometasone furoate and phospholipids (30–300 °C). Heat flow was recorded as the temperature change, and this process was performed separately for both the drug and excipients. Similarly, DSC analysis of the physical mixture was performed separately.

2.2.3 Determination of λmax of Mometasone Furoate by U.V Spectroscopy

2.2.3.1 Preparation of Stock Solution

A 10.0 mg (or 100 µg/ml) sample of mometasone furoate was precisely weighed and dissolved in a 100 ml V.F (volumetric flask) containing methanol. The concentration of the prepared stock solution was 0.1 mg/ml. In this way, a stock solution of mometasone furoate was prepared. The stock solution was further diluted to obtain the required concentrations of 2, 5, 8, 11, 14 µg/ml and 17µg/ml.

2.2.4Construction of Calibration Curve of MF

Using a UV-visible spectrophotometer, the absorbance of the different dilutions was measured at 248 nm with methanol as the blank. A standard curve was constructed with respect to concentration. The results are presented in **Table1**.

Table1: Observed values of different dilutions of mometasone furoate in methanol at 248 nm

Serial Number	Concentration (µg/ml)	Abs1	Abs2	Abs3	Average	SD (±)
1	2	0.145	0.139	0.143	0.142	0.003
2	5	0.297	0.299	0.298	0.298	0.001
3	8	0.463	0.465	0.458	0.462	0.003
4	11	0.616	0.619	0.617	0.617	0.001
5	14	0.779	0.785	0.781	0.782	0.003
6	17	0.965	0.966	0.973	0.968	0.004

2.2.3.5FTIR Analysis of MF, Phospholipids, Carbopol 934P, and Drug Excipient Compatibility Study using FTIR and FTIR analysis of the Optimized Formulation.

Spectra of pure MF, excipients (Phospholipid, Carbopol 934P), physical mixture of drug and excipients, and optimized nanoparticle gel formulation were analyzed using an FTIR spectrophotometer (Bruker Alpha, MA01821, USA). The quantity of the formulation ingredients in the physical mixture was similar to that of the optimized formulation. The pure drug, excipients, and physical mixture were then ground separately and combined with KBr at a ratio of 1:1by weight. Now, this (mixture) was pressed into a thin pellet, and its FTIR spectrum was recorded using a Fourier-Transform Infrared Spectrometer with a range of 4000 - 400 cm^{-1}.

2.2.3.6Formulation of Mometasone Furoate Phospholipid Complex

As shown in Table 2, accurately weighed amounts of mometasone furoate and phospholipids at various molar ratios were transferred into round-bottomed flasks, each containing 10 ml of solvent. Drug-phospholipid complexes were prepared by refluxing the dispersion at 80°C for six hours. Following reflux, the organic solvent was removed and the solution was converted into a thin film by rotary evaporation at 45°C and 80 rpm. The thin films were then dried overnight in a V.D (vacuum desiccator). The resulting drug-phospholipid complex was labeled and stored in a tightly sealed container until further use. For the current set of experiments, mometasone-phospholipid complexes were prepared using different solvents (methanol, ethanol, dichloromethane, and chloroform) at molar ratios of 0.01:0.01, 0.01:0.02, 0.01:0.03, 0.01:0.04, and 0.01:0.05.

Table 2:Composition of different solvents

Sr. No.	Formulation Code	Molar ratio (Mometasone furoate: Phospholipid)	Amount of mometasone (mg)	Amount of phospholipid (mg)	Solvents	Volume (ml)
1	F.1	0.01:0.02	56.10	151.60	Methanol	10
2	F.2	0.01:0.02	56.10	151.60	Ethanol	10
3	F.3	0.01:0.02	56.10	151.60	Chloroform	10
4	F.4	0.01:0.02	56.10	151.60	DCM	10
5	F.5	0.01:0.01	56.10	75.80	Ethanol	10
6	F.6	0.01:0.03	56.10	227.40	Ethanol	10
7	F.7	0.01:0.04	56.10	303.20	Ethanol	10
8	F.8	0.01:0.05	56.10	379.00	Ethanol	10

2.2.3.6.1 Characterization Mometasone Furoate Phospholipid Complex

2.2.3.6.1.1Physical Appearance

The physical appearance of all batches of mometasone furoate phospholipid complexes was analyzed by observing the visual clarity and colour of the solution.

2.2.3.6.1.2 Percentage Yield

The percentage yield of mometasone furoate phospholipid complexes was calculated as the ratio of the real amount of product obtained to the initial amount of the formulation.The formulated phospholipid complexes were carefully dried and weighed. The mass (weight) was divided by the total weight of the non-volatile drugs.

$$Percentage\ Yield\ (\%) = \frac{\text{Real Weight}}{\text{Initial Weight}} x100$$

2.2.3.6.1.3 Solubility of Complex in Water

The PL complex film was collected at various molar ratios, as shown in Table 2, and 5 ml of water was added to the vial containing the PL complex thin film and mixed thoroughly to ensure that the complex was uniformly distributed in water. The vial was then placed in a water-bath shaker. The mixture was agitated at a controlled speed (typically 100 rpm) for 24 h at 25±1.0°C to ensure equilibrium solubility. After 24 h, the complex sample was spun at 10,000 rpm for 15 min. to remove the insoluble particles from the solution. The supernatant was then accumulated and strained using a membrane filter with a 0.45µm pore size. The solubility of the compound in water was analyzed at 248 nm using a UV spectrophotometer.

2.2.3.6.1.4Percentage Drug Complexation and Drug Loading

Weighed 100 mg of MF-PL complex were added to 10 ml of ethanol to measure the drug complexation and loadingof mometasone furoate in phospholipid complexes. The dispersion was spun (centrifuged) at 15,000 rpm for 15 min. Following centrifugation, a clear liquid was obtained, and spectrophotometric analysis was used to estimate the percentage of drug complexation of free mometasone furoate at 248 nm. Drug complexation and loading were calculated using the following formula:

$$DC\ (\%) = \frac{\text{Final Weight}}{\text{Initial Weight}} x100$$

$$DL\ (\%) = \frac{\text{Final Weight}}{\text{Initial Weight}} x100$$

2.2.3.7 Preparation of Mometasone Furoate Phospholipid Nanoparticles

Accurate amounts of mometasone furoate and phospholipid (soy lecithin) were weighed according to the molar ratios specified in Table3. Ensured each formulation had the correct molar ratio of MF: PL (0.01:0.04).This weighed amount of mometasone furoate and phospholipid was transferred to separate round-bottom flasks. 10.0 ml of ethanol was added to each flask to obtain a homogeneous dispersion of the drug and phospholipid. A round-bottomed flask was set up on a reflux apparatus and the dispersion was heated to a constant temperature. of 80 °C for 6 h to facilitate the formation of mometasone furoate-phospholipid complex.After refluxing, the dispersion was transferred to a rotary evaporator. The rotary evaporator was operated at 45°C and 80 rpm. The solvent was evaporated to form a thin film of mometasone furoate phospholipid complexes on the walls of the RBF. Flasks containing the thin films were placed in a vacuum desiccator. The films were allowed to dry overnight to ensure that all residual solvents were removed.The drug-phospholipid complexes were labeled and stored in tightly closed containers to protect them from moisture and contamination.The dried thin films were rehydrated by placing the flask on a rotary machine. Next, 10 ml of water was added to each flask. Stir the mixture for 5 min. to ensure that the film was completely dispersed in water.A probe sonicator was used to sonicate the rehydrated film. The sonicator was set to a specified amplitude and time for each formulation.

F.7A1: 40% amplitude for 1 minute

F.7A2: 50% amplitude for 1 minute

F.7A3: 60% amplitude for 1 minute
F.7A4: 50% amplitude for 3 minutes
F.7A5: 50% amplitude for 5 minutes

An on-off cycle (4 s on and 5 s off) was used during sonication to ensure a uniform energy distribution and prevent overheating.

Table3: Composition of different formulation of MF-PL nanoparticle

Sr. No.	Formulation Code	MF: PL (in molar ratio)	Amplitude (%)	Time (min.)	Ethanol (ml)
1	F.7A1	0.01:0.04	40	1	10
2	F.7A2	0.01:0.04	50	1	10
3	F.7A3	0.01:0.04	60	1	10
4	F.7A4	0.01:0.04	50	3	10
5	F.7A5	0.01:0.04	50	5	10

2.2.3.7.1Characterization of Mometasone Furoate Phospholipid Nanoparticle

2.2.3.7.1.1 Visual Appearance

A small volume (2–5 ml) of each formulation was transferred to separate clean and clear glass vials. The vials were placed on a clean flat surface under uniform laboratory lighting. The samples were allowed to stand undisturbed for a specified time (24 h) to observe changes over time. Each vial was evaluated for the uniformity of dispersion.

2.2.3.7.1.2 Drug Entrapment Efficiency and Drug Loading

Weighed 100 mg of MF-PL nanoparticles were added to 10 ml of ethanol to measure the drug loading and complexation of mometasone furoate in phospholipid complexes. The dispersion was spun (centrifuged) at 15,000 revolution/min for 15 min, after which a clear liquid (supernatant) was obtained, and spectrophotometric analysis was used to estimate the percentage drug complexation quantity of free mometasone furoate (λmax = 248 nm). Drug complexation and DL were calculated using the following formulae:

$$EE\ \% = \frac{W_{(added\ drug)} - W_{(free\ drug)}}{W_{(added\ drug)}} \times 100$$

$$DL\ (\%) = \frac{\text{Final Weight}}{\text{Initial Weight}} x100$$

$W_{(added\ drug)}$= Amount of drug added
$W_{(free\ drug)}$ = Amount of free drug determined

2.2.3.7.1.3 Particle Size (PS) and Zeta Potential (ZP) Analysis

Employing a zeta sizer nano instrument (Model:ZS90), the PS and ZP of mometasone furoate phospholipid NPs were determined using dynamic light scattering and electrophoretic mobility, respectively. The prepared phospholipid nanoparticles were introduced into the sample holding unit and sample cell to assess PS and ZP, respectively.

2.2.3.7.1.4 TEM and SEM

Using TEM, morphology and structure of the mometasone furoate phospholipid nanoparticles were examined. The formulation was diluted 1:10 with water to conduct the T.E.M observations. After drying, a drop of the diluted solution was placed directly onto a 200-mesh C.C.C.G (carbon-coated Cu grid) and examined. Scanning electron microscopy (SEM) was used to reveal the morphology of mometasone furoate phospholipid nanoparticles.

2.2.3.8Formulation of Mometasone Furoate Loaded Phospholipid Nanoparticles Gel

The specific volume of the optimized formulation, which served as the base for the gel, was carefully measured. Carbopol 934P was gradually incorporated to the measured volume of the optimized formulation. Addition was performed carefully to avoid the formation of clumps and ensure uniform dispersion. Different formulations were prepared by varying the percentage of

Carbopol 934P to achieve the desired gel concentration. Typically, the concentrations tested were 0.5, 1, 1.5, and 2%. After Carbopol 934P was added, the mixture was stirred thoroughly until the Carbopol was completely dispersed. Once dispersion was complete, the mixture was left at room temperature for 24 h. During this time, the Carbopol powder swelled completely, which was essential for the gel to achieve its full viscosity and consistency. After swelling, the pH of the gel was adjusted to 6. This was achieved by adding a 1M NaOH solution dropwise while continuously stirring the gel. The pH was monitored using a pH meter and NaOH solution was added until the pH reached the desired level. NaOH solution was added in sufficient quantity (q.s) to obtain the desired pH (Table 4).

Table 4: Composition of different formulations of MF-loaded PL nanoparticlegel

Sr. No.	Ingredients	Formulation Code			
		F.7A4 (G-1)	F.7A4 (G-2)	F.7A4 (G-3)	F.7A4 (G-4)
1.	MF-Loaded Phospholipid Nanoparticle Solution (ml)	10.00	10.00	10.00	10.00
2.	Carbopol 934P (w/v)	0.50	1.00	1.50	2.00
3.	NaOH Solution (ml)	qs	qs	qs	qs

2.2.3.8.1 Characterization of Mometasone Furoate Loaded Phospholipid Nanoparticles Gel

2.2.3.8.1.1 Physical Appearance

The prepared MF-loaded PL nanoparticle gels were visually inspected to examine their physical properties, such as colour and uniformity.

2.2.3.8.1.2 pH

2.5 g of mometasone furoate loaded phospholipid nanoparticle gel was accurately weighed using a digital balance. The weighed gel was poured into a clean dry glass beaker. A volume of 25 ml of D.W was measured using a graduated cylinder and slowly poured into a glass beaker containing the gel. The gel and distilled water were mixed well. It was stirred with a glass rod until the gel completely dissolved in water and formed a uniform dispersion. The electrodes of the calibrated digital pH meter were immersed in the gel dispersion solution. The pH meter was allowed to stabilize, and the displayed pH value was recorded.

2.2.3.8.1.3 Viscosity

The viscosity of the prepared nanoparticles gel was measured using a Visco QC 100 viscometer. The gel was rotated at 24 rpm using spindle L4 at 25°C and the corresponding dial reading was recorded at each rotation.

2.2.3.8.1.4Spreadability

A spreadability study was conducted to assess the flow properties of the developed gel using the glass-plate method. A glass slide was pre-labeled or pre-marked, and 2 g T.S (test sample) of each gel was placed on a glass plate. The initial diameter of the gel was measured. Then, a second glass plate was placed over the first glass plate, and a 500 g weight was applied for 5 min. After this period, the final diameter of the gel spread was measured using a scale. The diameter values before and after applying the weights were recorded. Finally, the spreadability was calculated using these values in the appropriate equation.

$$Spreadability\ (S) = \frac{\text{Weight applied x (Final diameter} - \text{Initial diameter)}}{\text{Time taken (Seconds)}}$$

2.2.3.8.1.5Drug Content

One gram of each gel formulation was accurately weighed {F.7A4 (G-2), F.7A4 (G-3), and F.7A4 (G-4)}. Each 1 gram of gel was equivalent to 100 mg of mometasone furoate. A solution

of PBS, with a pH of 6.8. The solution was used as the dissolution medium. A weighed amount of each gel was transferred to a beaker. An appropriate amount of PBS (typically 25 ml) was added to each beaker containing the gel. The mixture was magnetically stirred until the gel was completely dispersed in PBS. It was ensured that there were no visible gel clumps and that the solution appeared homogeneous.The solution was filtered to remove undissolved particles. A suitable filter paper or membrane filter (Whatman No. 1 filter paper) was used to obtain a clear filter. The filtered solution was collected in a clean glass beaker. The absorbance of each sample solution (F.7A4(G-2), F.7A4(G-3), and F.7A4(G-4)) was measured at 248 nm.

2.2.3.8.1.6In Vitro Drug Release Assessment of Optimized Nanoparticles Gel

Absorbance readings of the control gel and optimized gel formulation at periodic intervals were recorded. The results are presented in Table 5.

Table 5: Observed values of control and optimized gel formulation {F.7A4 (G-2)} and their corresponding concentrations at different time intervals

Sr. No.	Time (Hrs.)	Absorbance (Control Gel)	Concentration of Control Gel (µg/ml)	Absorbance (Optimized Gel Formulation {F.7A4 (G-2)}	Concentration of Optimized Gel Formulation {F.7A4 (G-2)} (µg/ml)
1	0.25	5.824	106.194	28.319	518.2
2	0.5	18.901	345.699	55.496	1015.95
3	1	33.967	621.65	74.882	1371.00
4	2	48.425	886.45	93.755	1716.65
5	3	58.248	1066.35	110.391	2021.35
6	4	67.844	1242.1	131.663	2410.95
7	6	78.783	1442.45	159.173	2914.8
8	8	89.212	1633.45	174.049	3187.25
9	10	96.059	1758.85	191.963	3515.35
10	12	109.749	2009.6	243.307	4455.7

2.2.3.8.1.7Assessment ofDrug Release Kinetics of theOptimized Nanoparticles Gel

2.2.3.8.1.7.1 Zero orderkinetics

This zero-order equation, $C = C_0 + K_0t$, was applied to determine drug release from the optimized gel formulation {F.7A4 (G-2)} at different time intervals.C_0 = Initial drug concentration in the solution (usually equal to 0),C= Concentration of drug dissolved at time t, andK_0 = Zero-order release rate constant.

2.2.3.8.1.7.2 First order kinetics

The first-order equation is, $\log C = logC_0 - K.t/2.303$, was applied to determine drug release from the optimized gel formulation {F.7A4 (G-2)} at different time intervals. C = concentration of the drug remaining at time t,C_0 = initial drug concentration,K= First order rate constant and t = Time.

2.2.3.8.1.7.3 Higuchi's Model

The basic Higuchi equation is given by $Q = K_H . t^{1/2}$ was applied to determine drug release from the optimized gel formulation {F.7A4 (G-2)} at different SQRT (√t). K_H = Higuchi release constant, Q = cumulative amount of drug released at time t, and $t^{1/2}$ = square root of time. The drug release data were fitted to the Higuchi equation.

2.2.3.8.1.7.4 Korsmeyer-Peppas Model

The basic Korsmeyer-Peppasequation is given by$M_t/M_\infty = Kt^n$was applied to determine release rate of drug from the optimized gel formulation {F.7A4 (G-2)} at different log time intervals.M_t = amount of drug released at time t,M_∞ = totalamount of drug released at infinite time,K = release rate constant and$n$ = release exponent which indicates the mechanism of drug release.

2.2.3.9 In Vivo Study of Optimized {F.7A4 (G-2)} Nanoparticle Gel

For this study, 24 male Wistar rats, which were 8 to 9 weeks of age and weighed between 140 and 200 grams. Rats were housed in S.L.C (standard laboratory conditions) with a 12 h light/dark cycle, a temp. of 22 ± 2°C, and the RH of 55 ± 5%. They were provided free access to standard pellet diet and water and habituated for one week before the experiment(Ghasemi et al., 2021).

The 24 rats were unsystematically assigned into four groups, each consisting of six rats (Radin & Klinger, 1986): group 1 served as the control group and received no treatment; group 2 was given a gel base without the drug (placebo); group 3 received a free drug gel containing mometasone furoate without nanoparticles; and group 4 was treated with an optimized nanoparticle gel containing mometasone furoate-loaded phospholipid nanoparticles. The dorsal side of each rat was shaved to avoid skin damage, and the specific formulations were applied to the designated areas once daily for 7 days as follows: group 1 received no application, group 2 was treated with 1 g of placebo gel, group 3 received 1 g of free drug gel, and group 4 was treated with 1 g of optimized nanoparticle gel. Skin irritation and inflammation were observed at 24, 48, and 72 hours after the first application and then daily for 7 days of the study. Redness and inflammation of the skin were visually observed and scores were recorded (on Grading Scale 0 to 4) following the Draize procedure (Table6).This study followed a process authorized by the IAEC (IAEC/PH-23/TIPER/193 01/06/23).

Table 6: In-vivo observation sign of optimized {F.7A4 (G-2)} nanoparticle gel

Animal Group	Time Interval	Grading Scale (0-4)*		Observation
		Redness (Score)	Inflammation (Score)	
Group1: Control	24 h	0	0	No redness or inflammation observed
	48 h	0	0	No redness or inflammation observed
	72 h	0	0	No redness or inflammation observed
	7 days	0	0	No redness or inflammation observed
Group2: Placebo	24 h	1	1	Mild redness and inflammation observed
	48 h	1	0	Mild redness and inflammation diminished
	72 h	0	0	No redness or inflammation observed
	7 days	0	0	No redness or inflammation observed
Group3: Free Drug Gel	24 h	2	2	Moderate redness and inflammation observed
	48 h	2	1	Moderate redness with mild inflammation
	72 h	1	0	Mild redness and inflammation subsided
	7 days	0	0	No redness or inflammation observed
Group 4: Optimized Nanoparticle Gel	24 h	0	0	No redness or inflammation observed
	48 h	0	0	No redness or inflammation observed
	72 h	0	0	No redness or inflammation observed
	7 days	0	0	No redness or inflammation observed
Grading Scale: - 0: No redness/no inflammation; 1: mild redness/mild inflammation; 2: moderate redness/moderate inflammation; 3: Moderate to severe redness/moderate inflammation; 4: Severe redness to eschar formation/severe inflammation (raised more than 1 mm)				

2.2.3.10 Stability Assessment

The ICH Q1A (R2) stability guideline was used to determine the stability of the optimized nanoparticle gel. This is because ICH Q1A(R2) provides detailed information for the stability assessment of new pharmaceutical compounds and drug products, particularly gel-like dosage forms (Colgan et al., 2014). Stability studies were conducted for three months at scheduled time intervals of 0-day, 1, 2, and 3 months. The storage conditions were as follows (Roccato et al., 2017):

Room Temperature (RT)
Refrigerator (4±2°C)
25±2°C/60±5% RH
40±2°C/75±5% RH
The optimized {F.7A4 (G-2)} nanoparticles gel was stored in closed amber-coloured vials of glass, away from direct sunlight, under mention conditions for three months.

2.2.3.10.1 Organoleptic Properties

The visual appearance, colour, and odour of the optimized {F.7A4 (G-2)} gel formulation was observed at 0-day, 1-month, 2-month and 3-month time points and changes were noted. The results obtained were compared with the initial characteristics of the optimized nanoparticle gel recorded on day zero.

2.2.3.10.2 pH

Approximately 1 g of the optimized nanoparticle gel was weighed and diluted with 10 mL of distilled water. The pH values of the optimized nanoparticle gel formulation were measured at 0-day, 1-, 2-, and 3 months' time interval. The results obtained were compared with the initial pH of the optimized nanoparticle gel on zero day.

2.2.3.10.3 Spreadability

The spreadability stability of the optimized nanoparticle gel formulation was evaluated at intervals of 0 days, 1 month, 2 months, and 3 months. The obtained results were compared with the initial spreadability values of the optimized nanoparticle gel on 0-day.

2.2.3.10.4Percentage Drug Content

The % drug content of the optimized nanoparticle gel was measured at 0-day, 1, 2, and 3 months. The results obtained were compared with the % drug content of the optimized nanoparticle gel on 0-day.

2.2.3.10.5 Viscosity

The viscosity values of the optimized nanoparticle gel formulation were measured at 0-day, 1-month, 2-months and 3-months' time points. The results obtained were compared with the viscosity of the optimized nanoparticle gel on 0-day.

3.0Result and Discussion

3.1 Organoleptic properties

The powder was in crystalline form, indicating that no impurities were present in the powdered drug, and the colour was white to pale white, consistent with the expected appearance of pure mometasone furoate. No discoloration was observed, indicating that mometasone furoate was completely pure and authentic. No odour was observed for mometasone furoate, suggesting that it did not contain volatile impurities.

3.2 Melting point, Solubility and Partition coefficient (PC)

The MP of MF was in the range 219±1.0-225±1.0°C. It was clearly observed that mometasone furoate was slightly soluble in methanol (7.375±0.213 mg/mL), ethanol (6.392±0.055 mg/mL), and dichloromethane (DCM), and almost insoluble in phosphate buffer (PB, pH 6.8) and distilled water.The PC of mometasone furoate in n-octanol/water was determined to be; 4.19±0.385.

3.3 DSC Analysis of Drug (MF), Excipient (PL) and its Physical Mixture

DSC thermogram analysis revealed key thermal events, indicating the compatibility of mometasone furoate with phospholipids. In Fig.1 (a), mometasone furoate showed an onset temperature of 227.48°C with an endothermic peak at 229.65°C, marking its melting point without any significant recrystallization during cooling. In Fig.1 (b), the phospholipid phase exhibited two endothermic peaks: the first between 33.35°C and 94.98°C, indicating

phospholipid melting, and the second between 173.42°C and 219.15°C, suggesting potential crystallization or phase transitions. In Fig.1 (c), the mixture of mometasone furoate and phospholipids showed an initial melting event between 30.43°C and 96.31°C, followed by a second phase transition between 197.13°C and 208.94°C. The observed thermal behaviour indicated no major incompatibility between the components, indicating good compatibility in the physical mixture of MF and PL.

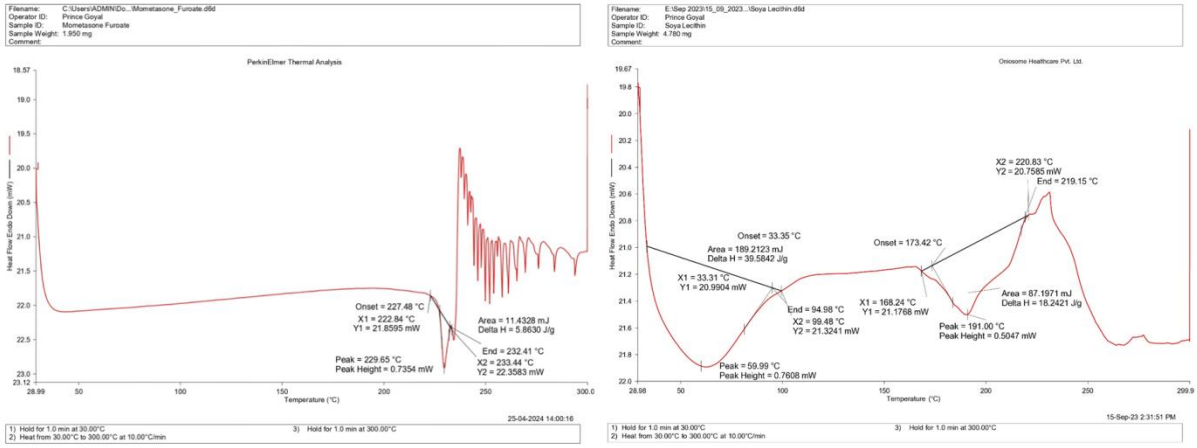

(a) (b)

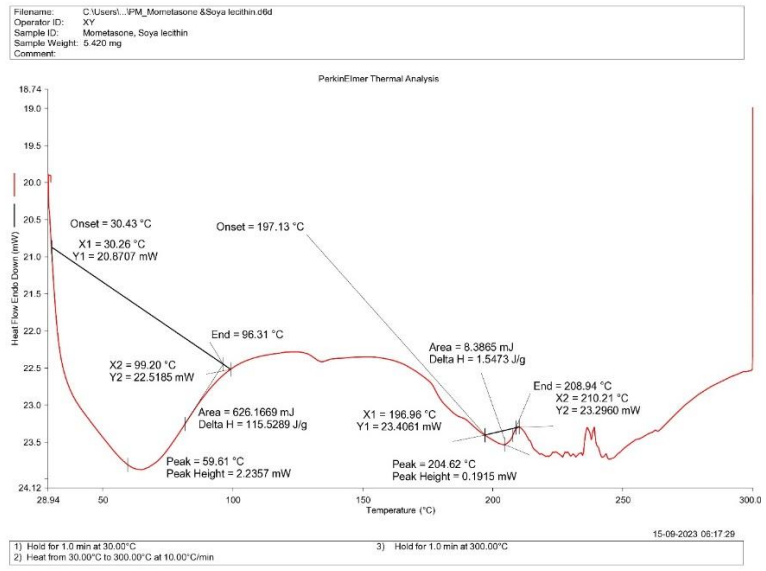

(c)

Fig.1:(a) DSC thermogram of MF (b) DSC thermogram of PLs (c) DSC thermogram of physical mixture (MF and PLs).

3.4 Determination of λmax and Construction of Calibration Curve

The λmax of mometasone furoate was 248 nm (Fig.2), similar to the reference standard. The consistent λmax at 248 nm at different concentrations suggests that the absorption peak is a specific property of the compound and is independent of concentration within the range studied. This λmax value was similar to the literature values for mometasone furoate, confirming the identity and purity of the compound used. The use of methanol as a solvent was appropriate because it did not interfere with absorbance in the UV range of interest. The high R^2 value confirmed that the UV-visible spectrophotometric technique was suitable for accurately estimating the concentration of mometasone furoate in methanol. The resulting standard calibration curve of mometasone furoate, as shown in the graph reflected by the

regression equation y = 0.0546 x + 0.0258, had a correlation coefficient (R^2) of 0.9991, indicating excellent linearity (Fig. 3).

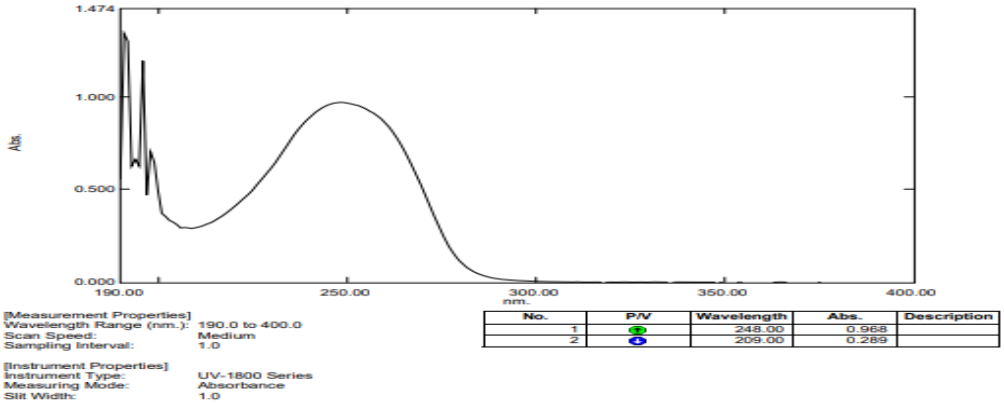

Fig.2: The UV spectrum of the MF.

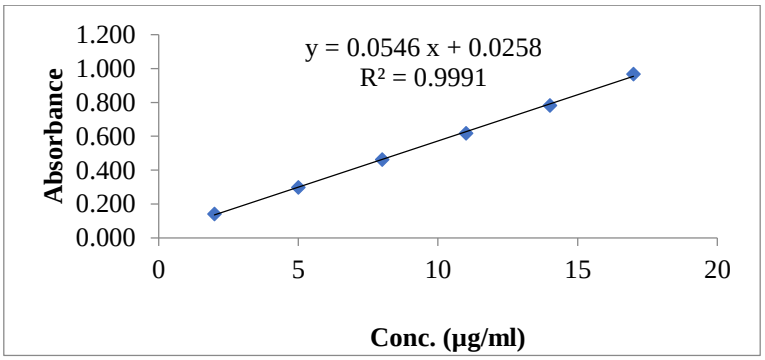

Fig.3: Calibration curve of mometasone furoate (in methanol).

3.5 FTIR Analysis{MF, PLs, Carbopol 934P, (Drug+Excipient), Optimized Formulation}

The F.T.I.R spectra of mometasone furoate, phospholipids, and Carbopol 934P are shown in Fig.4 **(a), (b),** and **(c).** The interpretation outcomes and major peaks of MF were observed at 1707.19 cm^{-1} (stretching of carbonyl group C=O),1619.18 cm^{-1} (stretching of C=C group), 1319.19 cm^{-1} (bending of C-H bond) and 1120.73 cm^{-1} (stretching of C-O group), 767.71 cm^{-1} all stretching of MF, which were identical to the cited peaks.

The primary signals (peaks) of phospholipids were observed at 3310.36 cm^{-1} (OH/NH stretching band) 2922.71 cm^{-1}, 2853.13 cm^{-1} (stretching band of C-H group) 1735.57 cm^{-1} (stretching band of C = O group), 1541.55 cm^{-1} (bending of N-H), 1464.73 cm^{-1} (CH_2/CH_3 bending), 1377.92 cm^{-1} (bending of C-H), cm^{-1} 1043.71 cm^{-1} (stretching band of P-O-C), 1227.23 cm^{-1} (P=O stretching), 816.11 cm^{-1} and 719.34 cm^{-1}(C-H out of plane bend) which confirmed the purity and genuineness of the phospholipid.

The prominent signal (peak) detected at 1698.92 cm^{-1} corresponds to the C=O stretching vibration, indicating the presence of carboxylic acid groups, which is characteristic of Carbopol 934P polymers.

The FTIR spectrum of the physical mixture of mometasone furoate (MF), phospholipid (PL), and Carbopol 934P displayed characteristic peaks for each component, including (O–H) stretching, (C–H) stretching, (C=O) stretching, and (C–O) stretching vibrations, as shown in Table 6. The spectrum (**d**) confirmed the presence of both drug and additives (PL, Carbopol 934P) peaks, indicating that the functional groups of each component were retained when combined. This suggests good compatibility between MF and the additives, with no significant chemical interactions.

The FTIR spectrum (**e**) revealed the presence of functional groups (FG) in the MF-loaded PL nanoparticle gel formulation. The main peaks were identified based on their corresponding functional groups. The interpreted values of the spectra with the reference peaks are mention in Table7.

Table 7: Interpretated values of FTIR spectra of the physicalmixture (MF, PL, and Carbopol 934P)

Observed Peak (cm^{-1})	Functional Group	Reference Peak (cm^{-1})	Reference Functional Group
3306.35	O-H Stretching (broad, hydrogen-bonded)	3300-3400	O-H Stretching (phospholipid)
2926.45	Stretching of C–H(Alkane)	2950	Stretching of C-H,phospholipid, Carbopol934)
2856.04	C-H Stretching(alkane)	2850	CH Stretching (phospholipid)
1637.81	Stretching of C=O (carboxylic acid)	1640-1658	C=O Stretching (mometasone furoate,Carbopol 934)
1466.76	CH bending (alkanes)	1460-1470	CH bending (phospholipid)
Interpreted values of FTIR spectra of the optimized gel formulation			
Observed Peak (cm^{-1})	**Functional Group**	**Reference Peak (cm^{-1})**	**Reference Functional Group**
3308.24	O-H Stretching	3200-3500	O-H (alcohols, phenols)
2925.62	C-H Stretching	2855-2950	Strong peak indicatingpresence of aliphatic C-H
2855.73	C-H Stretching	2855-2950	Additional CH stretching peak
1635.16	C=O Stretching	1600-1700	Sharp peak indicating presence of (C=O)group

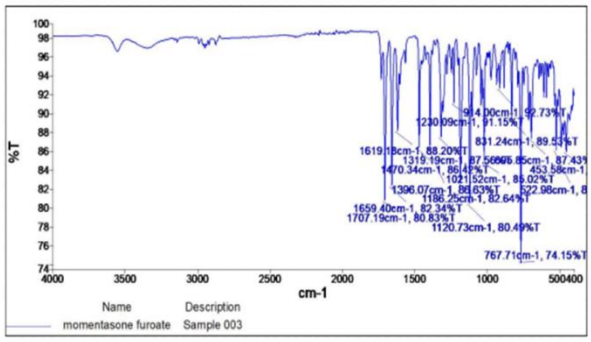

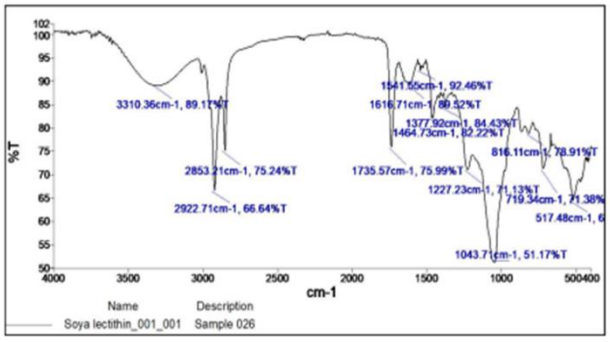

(a) (b)

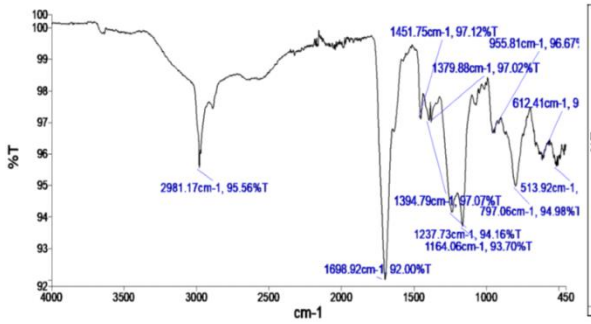

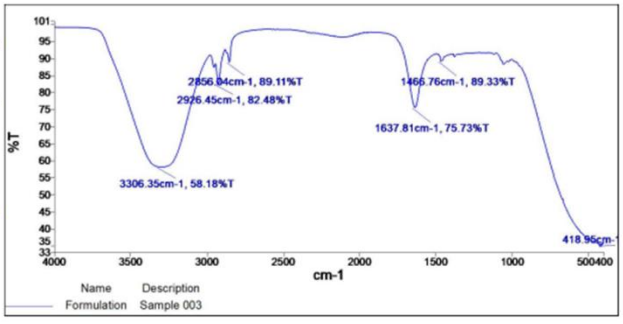

(c) **(d)**

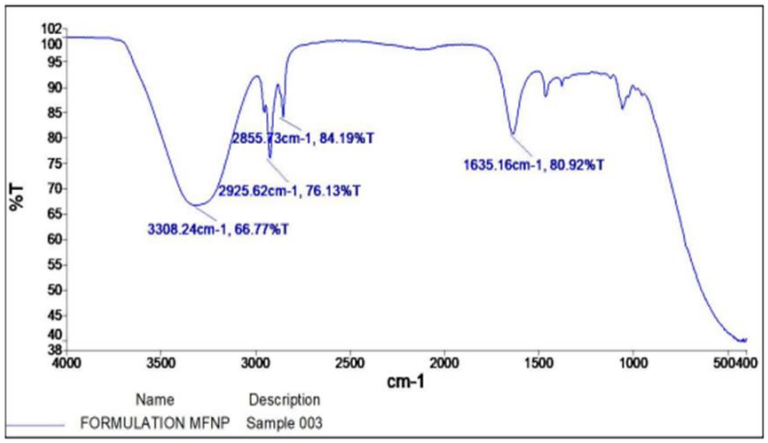

(e)

Fig.4: (a) F.T.I.R spectrum of MF (b) F.T.I.R spectrum of PL (c) F.T.I.R spectrum of Carbopol 934P (d) F.T.I.R spectrum of physical mixture (MF+PL+ Carbopol 934P) (e) F.T.I.R spectrum of optimized gel.

3.6 Formulated Mometasone Furoate Phospholipid Complex

The solubility of MF in aqueous media was significantly increased when it was formulated as a mometasone furoate-phospholipid complex. The solubility data in Table 2 shows a significant increase, which can be attributed to the formation of micelles.Complexation with phospholipids results in improved wetting and dispersion of MF, leading to enhanced solubility.At this stage, the mometasone furoate–phospholipid complex was formulated using the thin-film hydration technique. The observed increase in the solubility of mometasone furoate within the complex was attributed to the solubilization effect arising from micelle formation in the medium and the amorphous nature of the complex.In this study, mometasone furoate-phospholipid complex (MF-PL) was prepared to act as an intermediate with improved lipophilicity. Various solvents have been utilized to evaluate the solubility of drugs and phospholipids in different ratios within the complex. The final complex formulation was selected based on comprehensive evaluation studies.

3.6.1 Characterized Mometasone Furoate Phospholipid Complex

3.6.1.1 Physical Appearance

The results showed that the prepared mometasone furoate phospholipid complexes in all batches were uniform in shape and size (Table8 and Fig.5). This is important for achieving consistent dosing and bioavailability.

3.6.1.2 Percentage Yield

As shown in Table 8, the % yields of all the formulations were in the range of 92.260±0.782% to 96.260±0.844%. Formulation F.7 showed the highest yield of 96.260±0.844%,indicating that the process conditions were optimal for this particular formulation.

3.6.1.3 Solubility of Complex in Water

The solubility profile of the MF-PL complex in water was analyzed using different formulations (F.1–F.8). The solubility varied from 0.012 mg/ml in formulation F.1 to a maximum of 0.041 mg/ml in formulation F.7.These values are mention in Table 8.

3.6.1.4 Percentage Drug Complexation and Drug Loading

As shown in Table 8 and Fig.8, percentage drug complexation in all formulations ranged from 63.030±0.268% to 94.490±0.054%. Formulation F.7 exhibits the highest entrapment efficiency or drug complexation (94.490 ± 0.054%), indicating that this formulation was the most effective in loading mometasone furoate within the phospholipid complex.

The percentage of drug loading of the mometasone furoate-phospholipid complex in the different formulations (F.1–F.8) was significantly different. Formulation F.7 showed the

highest drug loading (36.67%), while formulation F.8 had the lowest loading (11.55%). The values are listed in Table 8.

Fig. 5: Visual appearance ofMF-PLs complex.

Table 8:Physical appearance, (%) yield, solubility, (%) drug complexation and (%) drug loading of mometasone furoate phospholipid complex

Serial Number	Formulation Code	Physical Appearance	(%) Yield	Solubility (mg/ml)	(%) Drug Complexation	(%) Drug Loading
1.0	F.1	Thin-Film	93.930±0.750	0.012±0.001	63.030±0.268	16.210±0.202
2.0	F.2	Thin-Film	95.070±0.750	0.025±0.001	90.260±0.070	23.910±0.168
3.0	F.3	Thin-Film	94.910±0.750	0.018±0.001	74.160±0.352	19.990±0.067
4.0	F.4	Thin-Film	95.730±0.491	0.016±0.001	76.270±0.176	20.380±0.091
5.0	F.5	Thin-Film	92.260±0.782	0.023±0.003	84.580±0.352	16.180±0.089
6.0	F.6	Thin-Film	95.650±0.547	0.036±0.002	89.170±0.073	18.210±0.111
7.0	F.7	Thin-Film	96.260±0.844	0.041±0.001	94.490±0.054	36.670±0.082
8.0	F.8	Thin-Film	95.490±0.584	0.039±0.001	92.030±0.088	11.550±0.091

3.7 Prepared Mometasone Furoate Phospholipid Nanoparticles

Different formulations (F.7A1 to F.7A5) of mometasone furoate phospholipid nanoparticles were prepared by varying the sonication amplitude and time, while maintaining the molar ratio of mometasone furoate and the volume of ethanol constant. Increasing the sonication time at a moderate amplitude further reduced the nanoparticle size and improved the homogeneity compared with F.7A2.

3.7.1 Characterized Mometasone Furoate Phospholipid Nanoparticle

3.7.1.1 Visual Appearance

All five formulations of mometasone furoate phospholipid nanoparticles (F.7A1, F.7A2, F.7A3, F.7A4, and F.7A5) exhibited homogeneous dispersion with no signs of phase separation. The visual appearance of the mometasone furoate-loaded phospholipid nanoparticle formulation is shown in Fig.6, and the results are presented in Table9.

Fig.6:Visual appearance ofMF-PL nanoparticles.

3.7.1.2 Drug Entrapment Efficiency and Drug Loading

As shown in Table 9, the % of drug entrapment in all formulations ranged from 82.683±0.269% to 94.412±0.215%. These findings indicated that phospholipid concentration has a major effect on the % of drug entrapment. As shown in Table 9, the % of drug entrapment increased with increasing phospholipid concentrations. However, this increase occurred after a threshold concentration of phospholipids was reached, beyond which no further increase in percent entrapment was observed. The maximum percentage of drug entrapment was found in formulation F.7A4, which was 94.412 ± 0.215%.

The % drug loading of mometasone furoate phospholipid nanoparticle formulations ranged from 15.98 ± 0.156% to 16.82 ± 0.128%. The highest drug loading was recorded for formulation F.7A4 (16.82 ± 0.128%), whereas the lowest was recorded for formulation F.7A1 (15.98 ± 0.56%) (Table 9). The observed data indicated that the percentage of drug loading in different formulations of mometasone furoate-loaded phospholipid nanoparticles was relatively consistent with a narrow range of variation.

Table 9: Visual appearance, percentage entrapment efficiencyand percentage drug loading of various MP-PL nanoparticle formulations

Serial Number	Formulation Code	Visual Appearance	(%) Entrapment Efficiency	(%) Drug Loading
1.0	F.7A1	Homogeneous dispersion with no phase separation form	91.664±0.367	15.98±0.156
2.0	F.7A2	Homogeneous dispersion with no phase separation form	93.073±0.667	16.75±0.163
3.0	F.7A3	Homogeneous dispersion with no phase separation form	85.853±0.443	16.36±0.057
4.0	F.7A4	Homogeneous dispersion with no phase separation form	94.412±0.215	16.82±0.128
5.0	F.7A5	Homogeneous dispersion with no phase separation form	82.683±0.269	16.45±0.053

3.7.1.3 Particle Size (PS) and Zeta Potential (ZP)

The F.7A4 formulation exhibited a sharp particle size distribution peak with a hydrodynamic diameter of 191.60 nm, confirming the successful development of nanoparticles. The polydispersity index (PDI) was 21.9%, indicating moderate particle size uniformity (Fig.7). The zeta potential (ZP) measured at -37.5 mV, with a narrow standard deviation of ±0.7 mV, signified high formulation stability. Additionally, the consistent surface charge distribution, reflected by a peak at -35.2 mV and electrophoretic mobility of -2.6874 µm cm/Vs, further reinforced the stability and uniformity of the nanoparticles (Fig.8).

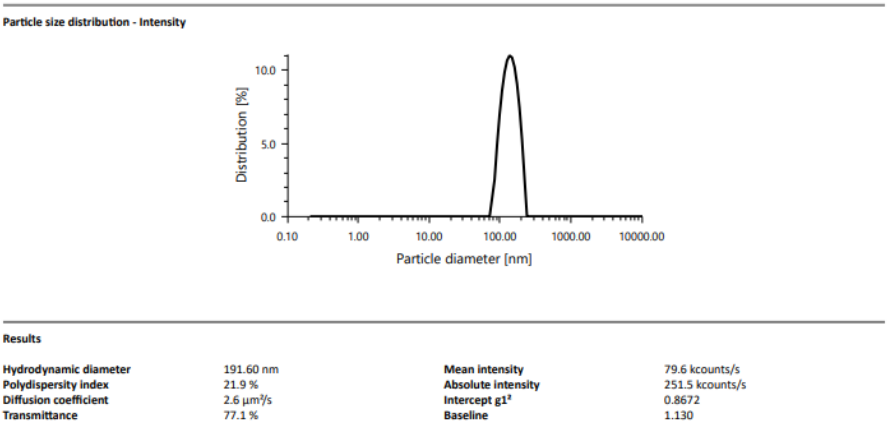

Fig.7: Particle size peak of F.7A4 formulation.

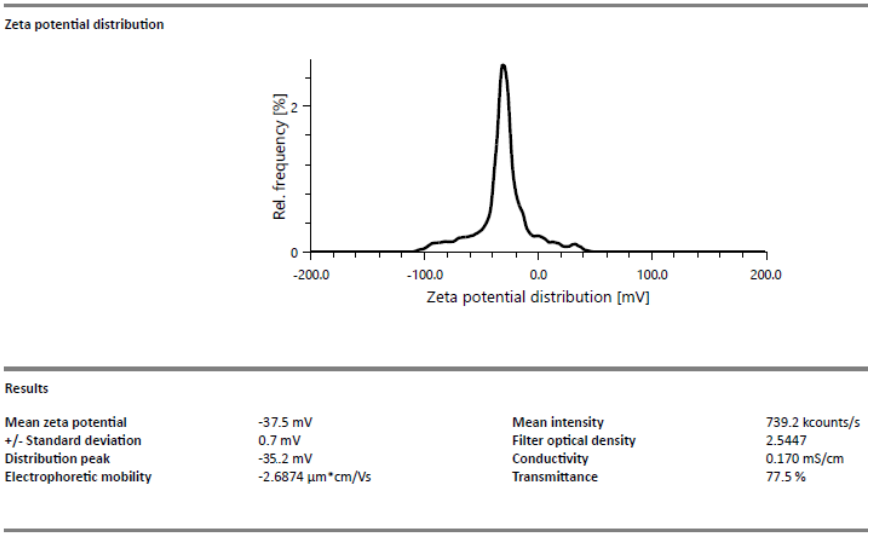

Fig.8: Zeta potential graph of F.7A4 formulation.

3.7.1.4 TEM and SEM

TEM images of mometasone furoate-loaded phospholipid nanoparticles (F.7A4) showed well-defined, smooth, and uniformly sized particles, all within the nanometre range, with individual particles less than 100 nm in diameter (Fig.9 a). In contrast, SEM images revealed that the same optimized formulation exhibited a smooth surface texture and a range of particle sizes, from small to large aggregates, with particles predominantly in the micrometre range of 0.01–0.1 µm in diameter (Fig.9 b).

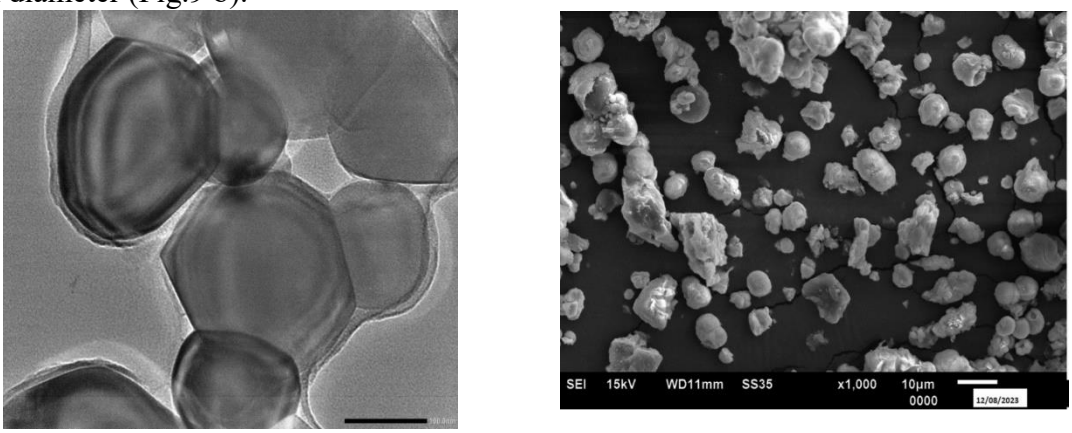

Fig.9(a): TEM image of F.7A4 formulation.(b) SEM image of F.7A4 formulation.

3.8 Formulated Mometasone Furoate Loaded Phospholipid Nanoparticles Gel

The different formulations (F.7A4 (G-1), F.7A4 (G-2), F.7A4 (G-3), and F.7A4 (G-4)) were successfully prepared using varying concentrations of Carbopol 934P. The pH of all the formulations was adjusted to 6. F.7A4 (G-2) formulation successfully formed a uniform gel, indicating that the components and conditions were optimal.

3.8.1 Characterization of Mometasone Furoate Loaded Phospholipid Nanoparticle Gel

3.8.1.1 Physical Appearance

The different formulations of MF-loaded PL nanoparticle gels exhibited different physical characteristics (Fig.10). The results obtained after observing the MF-loaded PL nanoparticle gel formulations are presented in Table 10.

Table10: Physical observation of MF- loaded PL nanoparticle gel

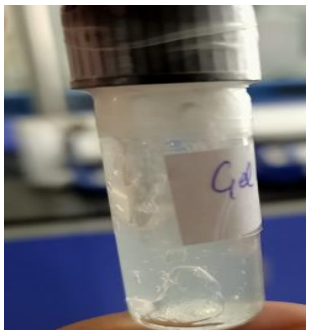

Serial Number	Formulation Code	Physical Appearance
1.0	F.7A4 (G-1)	No Gel Formed
2.0	F.7A4 (G-2)	Gel Formed (Uniformed)
3.0	F.7A4 (G-3)	Gel Formed (Sticky)
4.0	F.7A4 (G-4)	Gel Formed (Sticky)

Fig.10: Physical appearance of MF-loaded PL nanoparticle gel (F.7A4 (G-2).

3.8.1.2 pH

The pH of the different formulations was essential to ensure the stability and efficacy of the MF-loaded PL nanoparticle gel, as well as their compatibility with skin application. Formulation F.7A4 (G-2) showed the highest pH (6.24 ± 0.031) among the three formulations (Table 11).

3.8.1.3 Viscosity

The viscosity of the MF-loaded phospholipid nanoparticle gel formulation F.7A4 (G-2) was 2444 ± 2.08 cps, indicating optimal viscosity among the three formulations. This suggests a less dense gel matrix, potentially allowing faster drug release and improved spreadability (Table11).

3.8.1.4 Spreadability

The spreadability of the MF-loaded phospholipid nanoparticle gel formulations was varied, with F.7A4 (G-2) showing the highest spreadability at 7.23 ± 0.021 g.cm/sec, indicating ease of application. F.7A4 (G-3) had the lowest spreadability at 7.17 ± 0.015 g.cm/sec.These differences reflect the balance between viscosity and spreadability, which is crucial for optimizing the gel performance and patient compliance (Table11).

3.8.1.5 Drug Content

The % drug content of various mometasone furoate-loaded phospholipid nanoparticle gel formulations, as detailed in Table 11, revealed that formulation F.7A4 (G-2) had the highest drug content of 98.535%, indicating efficient drug incorporation with minimal loss during formulation. The low standard deviation (±0.366) showed consistency in drug loading in different formulations.

Table 11: pH, viscosity, spreadability, and percentage drug content of various MF-loaded PL nanoparticle gels.

Serial Number	Formulation Code	pH (Mean±SD)	Viscosity(cps) (Mean ± SD)	Spreadability (g.cm/sec) (mean ± SD)	%Drug Content
1.0	F.7A4 (G-2)	6.24±0.031	2444±2.08	7.23±0.021	98.535±0.366
2.0	F.7A4 (G-3)	6.12±0.023	2965±1.53	7.17±0.015	95.299±0.693
3.0	F.7A4 (G-4)	6.14±0.038	2885±1.53	7.18±0.026	94.505±0.317

3.8.1.6 In Vitro Drug Released

The in vitro drug release of the optimized mometasone furoate-loaded phospholipid nanoparticle gel {F.7A4 (G-2)} and the control gel were studied, as shown in Table 12 and Fig.11. The in vitro drug release assessment of the MF-loaded PL nanoparticle gel (F.7A4 (G-2) and the control gel was conducted for a period of 12 h. The data revealed that the optimized nanoparticle gel formulation F.7A4 (G-2) released significantly more drug than the control gel at all the measured time points.

Table12: In vitro drug release values of the control geland optimizednanoparticle gel formulations

Serial Number	Time (Hrs.)	% Drug Release ofControl Gel	% Drug Release of Optimized Nanoparticles Gel {F.7A4 (G-2)}
1.0	0.25	2.124±0.009	10.364±0.054
2.0	0.5	6.914±0.054	20.319±0.161
3.0	1	12.433±0.903	27.420±0.105
4.0	2	17.729±0.088	34.333±0.191
5.0	3	21.327±0.073	40.427±0.885
6.0	4	24.841±0.073	48.219±0.793
7.0	6	28.849±0.113	58.296±0.268
8.0	8	32.669±0.088	63.745±0.617
9.0	10	35.176±0.162	70.307±0.930
10	12	40.192±0.507	89.114±0.249

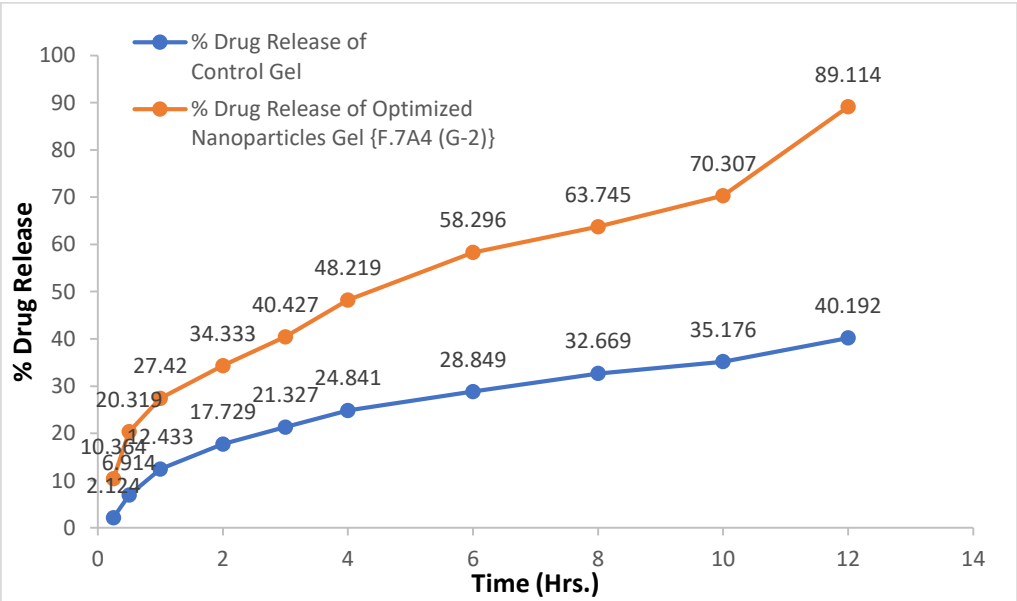

Fig. 11: (%) drug release of the control gel and optimized {F.7A4 (G-2)}

nanoparticles gel.

3.8.1.7Drug Release Kinetics of Optimized Nanoparticles Gel Formulation

The optimized nanoparticle gel showed a steady drug release rate of 6.2027% per hour, following zero-order kinetics, as indicated by the high COD (R^2 = 0.9248). Drug release also fit a first-order kinetic model (R^2 = 0.9053), with a slope of -0.0619, indicating a decrease in the log percentage of drug remaining over time. The Higuchi model (R^2 = 0.9801) confirmed that the drug release was primarily controlled by diffusion. The Korsmeyer-Peppas model (R^2 = 0.9777) further supported this, with an n value of 0.4873, indicating Fickian diffusion as the release mechanism.

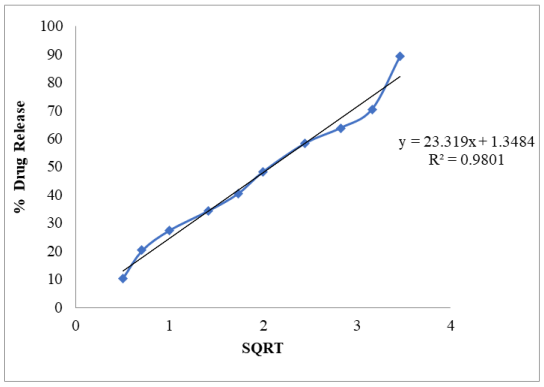

Fig.14: Higuchi graph of optimized nanoparticles gel {F.7A4 (G-2)}.

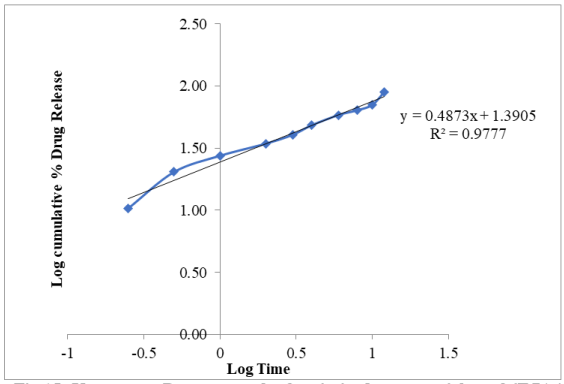

Fig.15: Korsmeyer-Peppas graph of optimized nanoparticles gel {F.7A4 (G-2)}.

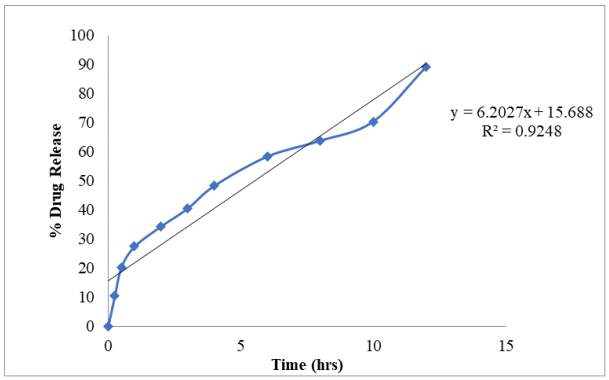

Fig.12: Zero order release of optimized nanoparticles gel {F.7A4 (G-2)}.

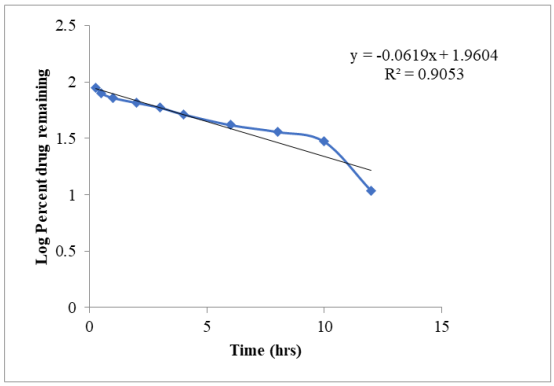

Fig.13: First order release of optimized nanoparticles gel {F.7A4 (G-2)}.

The R^2 value was determined for each plot, and is presented in Table 13 and Fig. 12–15. The Higuchi model, with an R^2 value of 0.980, best fit the release data. These results indicate that the drug diffused from the mometasone furoate-loaded phospholipid nanoparticle gel in a sustained manner.

Table 13:Kinetic equation parameter of optimized nanoparticles gel formulation {F.7A4 (G-2)}

FC	Zero order		First order		Higuchi		K. Peppas	
	K_0	R^2	K	R^2	K_H	R^2	K	R^2
F.7A4 (G-2)	6.2027	0.9248	-0.0619	0.9053	23.319	0.9801	0.4873	0.9777

3.9In Vivo Study of Optimized {F.7A4 (G-2)} Nanoparticle Gel

The results recorded showed that optimized mometasone furoate-loaded phospholipid nanoparticle gel was non-irritating and non-inflammatory to the skin. Throughout the study, no

signs of erythema (redness) or inflammation (edema) were observed in group 1 (control). The placebo (group 2) initially showed mild skin irritation, possibly due to the mechanical effect of the gel base, which diminished during the study period. Group 3 (free drug gel) showed moderate redness and mild inflammation, especially at 24 h and 48 h, which subsided by day 7. In contrast, group 4 (nanoparticle gel) showed no redness or inflammation, similar to that of the control group. This indicated that the mometasone furoate-loaded phospholipid nanoparticle gel formulation was well tolerated on rat skin.

3.10Stability

The results indicated that the optimized nanoparticle gel was smooth, clear, and odourless. They were uniformly light creamish in colour with no evidence of lump formation. The pH and spreadability remained consistent under all storage conditions at 0 days, 1 month, 2 months and during 3 months stability study. The percentage drug content and viscosity of the optimized nanoparticle gel were also consistent over a period of three months under all storage conditions. The observed changes in viscosity were minimal and within the standard deviation limits, indicating the good stability of the gel (Table 14).

Table 14: Effect of storage conditions on organoleptic properties, pH, spreadability, drug content, and viscosity of the optimized nanoparticle gel

Duration (Days)	Storage condition	Visual Appearance	Colour	Odour	pH	Spreadability (g.cm/sec) (Mean ±SD)	Drug Content (%) (Mean ±SD)	Viscosity (cps) (Mean ±SD)
0 Days	Control (RT)	C. C. G	Light creamish colour	(-)	6.253±0.015	7.655±0.002	98.230±0.280	2446.3±2.517
0 Days	Refrigerator 4±2°C	C.C. G	Light creamish colour	(-)	6.283±0.006	7.415±0.003	98.779±0.280	2451.0±2.000
0 Days	25±2°C/60±5% RH	C.C. G	Light creamish colour	(-)	6.243±0.015	7.654±0.004	98.962±0.381	2446.3±2.887
0 Days	40±2°C/75±5% RH	C.C. G	Light creamish colour	(-)	6.213±0.021	7.773±0.002	98.718±0.366	2441.0±2.082
1 Month	Control (RT)	C. C. G	Light creamish colour	(-)	6.257±0.015	7.656±0.004	98.718±0.183	2445.7±2.082
1 Month	Refrigerator 4±2°C	C. C. G	Light creamish colour	(-)	6.273±0.015	7.418±0.003	98.901±0.189	2452.0±1.000
1 Month	25±2°C /60±5% RH	C. C. G	Light creamish colour	(-)	6.240±0.010	7.657±0.002	98.962±0.280	2447.3±2.887
1 Month	40±2°C/75±5% RH	C. C. G	Light creamish colour	(-)	6.213±0.006	7.774±0.003	98.474±0.381	2440.7±3.215
2 Months	Control (RT)	C. C. G	Light creamish colour	(-)	6.257±0.012	7.652±0.003	98.962±0.461	2445.3±2.517
2 Months	Refrigerator 4±2°C	C. C. G	Light creamish colour	(-)	6.280±0.010	7.411±0.002	98.840±0.763	2450.0±2.000
2 Months	25±2°C /60±5% RH	C. C. G	Light creamish colour	(-)	6.247±0.006	7.659±0.002	98.779±0.461	2445.3±2.887
2 Months	40±2°C/75±5% RH	C. C. G	Light creamish colour	(-)	6.233±0.025	7.779±0.002	98.901±0.317	2439.3±2.082

3 Months	Control (RT)	C. C. G	Light creamish colour	(-)	6.233±0.015	.648±0.002	98.230±0.280	2446.0±1.000
3 Months	Refrigerator 4±2°C	C. C. G	Light creamish colour	(-)	6.280±0.010	7.418±0.003	98.718±0.485	2452.3±1.528
3 Months	25±2°C /60±5% RH	C. C. G	Light creamish colour	(-)	6.243±0.015	7.657±0.002	98.779±0.280	2445.3±2.517
3 Months	40±2°C/75±5% RH	C. C. G	Light creamish colour	(-)	6.213±0.015	7.776±0.003	98.840±0.280	2442.0±1.000

Note: {C.C.G = Creamish Clear Gel; (+) = Bad Odour Produced, (-) = No bad Odour}

Conclusion

The crystalline form of mometasone furoate indicates its stability and purity, as the lack of discoloration and absence of odour suggest no impurities. The melting point of the drug, found to be, aligns with the literature values, further confirming its identity and purity. Mometasone furoate is slightly soluble in methanol, ethanol, and dichloromethane (DCM) but is almost insoluble in PB and distilled water. The partition coefficient was satisfactory, indicating its lipophilic nature. The DSC analysis showed that the onset and peak temperatures of melting were 227.48°C and 229.65°C, respectively. Two distinct endothermic peaks in the phospholipid DSC thermogram suggested melting and possible crystallization or phase transitions.

UV-visible spectrophotometric analysis confirmed the λmax of mometasone furoate at 248 nm, showing excellent linearity with a high R^2 value, indicating the suitability of this method for concentration estimation.FTIR spectra confirmed the purity and authenticity of mometasone furoate by identifying characteristic peaks of its functional groups. Similarly, the FTIR spectra of phospholipid and carbopol 934P validated their composition by matching known reference positions. The FTIR spectra of the physical mixtures indicated compatibility among the components.The mometasone furoate-phospholipid complex, formulated using thin-film hydration, showed increased solubility, stability, and bioavailability. The nanoparticle formulations exhibited a homogeneous dispersion and physical stability. Formulation F.7A4 demonstrated excellent stability with negative zeta potential and hydrodynamic diameter. TEM and SEM images confirmed the uniform shape, smooth surface texture, and nanometer-sized particles.The physical appearance, pH, viscosity, spreadability, and drug content of the MF-loaded PL nanoparticle gels were assessed. Formulation F.7A4 (G-2) formed a uniform gel with a suitable pH, viscosity, and high spreadability. It also had the highest drug content, with minimal deviation, indicating efficient incorporation and consistency in the formulation.

Overall, this study concluded that mometasone furoate-phospholipid nanoparticle gel was successfully formulated and can be employed in the treatment of psoriasis and skin dermatitis with minimal side effects.

Summery

The "**development and characterization of novel nanoparticulate gel formulations for the state-of-the-art treatment of skin disease**" are highly promising and multi-dimensional.The successful completion of this study could lead to key innovations in topical drug delivery systems, mainly for the treatment of skin problems. The objective of this study was to enhance the therapeutic efficacy and patient outcomes of mometasone furoate-loaded phospholipid nanoparticle gel, focusing on improving its loading and permeability. The development and characterization of this complex, as well as its formulation in nanoparticle gels, are expected to provide many benefits. Optimized formulations can lead to improved drug release profiles, ensuring consistent and prolonged therapeutic effects, thereby improving skin condition management and potentially accelerating treatment times. Increasing the drug loading capacity

and skin penetration may allow lower doses and less frequent use, thereby reducing side effects and improving patient compliance. The methodology developed can be applied to other lipophilic drugs, extending nanoparticulate gel technology to treat various dermatological conditions and localized diseases.

By providing a more convenient route of administration and reducing the need for frequent applications, this novel formulation is likely to enhance patient compliance to treatment regimens, thereby improving overall results.Conducting stability studies ensured that the nanoparticulate gel remained effective and safe over time, which is important for commercial feasibility and clinical use.

Acknowledgment

The authors wish to extend their heartfelt gratitude to Prof. Md Arif Naseer, Adarsh Vijendra Institute of Pharmaceutical Sciences, Shobhit University, for his guidance and support throughout this research.

Conflict of Interest

The authors declare that they have no conflicts of interest related to this study.

Funding Sources

This study received no sponsorship or financial support from any governmental or industrial organizations.

References

1.Taléns-Visconti, R., Perra, M., Ruiz-Saurí, A., &Nácher, A. (2022). New Vehiculation Systems of Mometasone Furoate for the Treatment of Inflammatory Skin Diseases. Pharmaceutics, 14(12), 2558. https://doi.org/10.3390/pharmaceutics14122558

2.Basra, M. K., & Shahrukh, M. (2009). Burden of skin diseases. Expert Review of Pharmacoeconomics & Outcomes Research, 9(3), 271–283. https://doi.org/10.1586/erp.09.23

3.Karole, S., Chakraborty, A. K., Sagar, A., &Loksh, K. R. (2022). Formulation, development and characterization of topical organogel of mometasone furoate for the treatment of skin disease. Indian Journal of Pharmacy and Pharmacology, 9(1), 51–56. https://doi.org/10.18231/j.ijpp.2022.009

4.Spada, F., Barnes, T. M., & Greive, K. A. (2018). Comparative safety and efficacy of topical mometasone furoate with other topical corticosteroids. Australasian Journal of Dermatology, 59(3), e168–e174. https://doi.org/10.1111/ajd.12762

5.Branco, A. C. C. C., Sato, M. N., Pietrobon, A. J., & Yoshikawa, F. S. Y. (2018). Role of Histamine in Modulating the Immune Response and Inflammation. Mediators of Inflammation, 2018(6), 1–10. https://doi.org/10.1155/2018/9524075

6.Lee, J., &Burckart, G. J. (1998). Nuclear factor kappa B: important transcription factor and therapeutic target. The Journal of Clinical Pharmacology, 38(11), 981–993. https://doi.org/10.1177/009127009803801101

7.Marone, G. (1995). Human Basophils and Mast Cells. karger.https://doi.org/10.1159/isbn.978-3-318-01668-0

8. Patravale, V. B., &Mandawgade, S. D. (2008). Novel cosmetic delivery systems: an application update. International Journal of Cosmetic Science, 17(1), 41-56. https://doi.org/10.1111/j.1468-2494.2008.00416.x

9. Ho Lee, J. (2014). Nanoparticle-assisted Controlled Drug Release. Journal of Nanomedicine & Biotherapeutic Discovery, 04(02). https://doi.org/10.4172/2155-983x.1000e133

10. Archana, Niranjan, A. K., & Gupta, S. (2022). A Comprehensive Review on In-Situ Gel Drug Delivery System. Journal of Drug Delivery and Therapeutics, 12(4-S), 245–248. https://doi.org/10.22270/jddt.v12i4-s.5539

11. Xu, Q., Min, D., Petr, R., Parikh, V., & Tan, S. (2020). Clarification of the USP compendial procedure for phenoxybenzamine hydrochloride via updating impurity profiles. Journal of Pharmaceutical and Biomedical Analysis, 191, 113618. https://doi.org/10.1016/j.jpba.2020.113618
12. Colgan, S. T., Fields, K. W., Timpano, R. J., Roberts, M., Scrivens, G., Ryan, K., & Weaver, R. (2014). Opportunities for Lean Stability Strategies. *Journal of Pharmaceutical Innovation*, *9*(4), 259–271.
13. Roccato, A., Uyttendaele, M., &Membré, J.-M. (2017). Analysis of domestic refrigerator temperatures and home storage time distributions for shelf-life studies and food safety risk assessment. *Food Research International*, *96*, 171–181.
14. Ghasemi, A., Jeddi, S., & Kashfi, K. (2021). The laboratory rat: Age and body weight matter. *EXCLI Journal*, *20*(1). https://doi.org/10.17179/excli2021-4072
15. Radin, N. S., & Klinger, P. (1986). A computer program for selecting animals for control and experimental groups in biochemical studies. *Bioinformatics*, *2*(2), 107–109. https://doi.org/10.1093/bioinformatics/2.2.107
16. Lambrechts, I. A., de Canha, M. N., & Lall, N. (2018). Exploiting medicinal plants as possible treatments for acne vulgaris. In medicinal plants for holistic health and well-being 117-143. https://doi.org/10.1016/B978-0-12-812475-8.00004-4
17. Chang, E. H., Harford, J. B., Eaton, M. A. W., Boisseau, P. M., Dube, A., Hayeshi, R., Swai, H., & Lee, D. S. (2015). Nanomedicine: Past, present and future – A global perspective. Biochemical and Biophysical Research Communications. https://doi.org/10.1016/j.bbrc.2015.10.136
18. Gao, W., Zhang, Y., Zhang, Q., & Zhang, L. (2016). Nanoparticle-hydrogel: A hybrid biomaterial system for localized drug delivery. Annals of Biomedical Engineering, 44(6), 2049–2061. https://doi.org/10.1007/s10439-016-1583-9
19.Chen, Y., Chen, H., & Shi, J. (2013). In vivo bio-safety evaluations and diagnostic/therapeutic applications of chemically designed mesoporous silica nanoparticles. Advanced Materials, 25(23),3144-3176. https://doi.org/10.1002/adma.201205292
20. van Hoogevest, P., & Wendel, A. (2014). The use of natural and synthetic phospholipids as pharmaceutical excipients. *European Journal of Lipid Science and Technology, 116*(9), 1088-1107. https://doi.org/10.1002/ejlt.201400219
21. Ullah Khan, S., Saleh, T. A., Wahab, A., Khan, M. H. U., Khan, D., Ullah Khan, W., Rahim, A., Kamal, S., Ullah Khan, F., & Fahad, S. (2018). Nanosilver: New ageless and versatile biomedical therapeutic scaffold. International Journal of Nanomedicine, 13, 733-762. https://doi.org/10.2147/IJN.S153167
22. Nowacek, A., Kosloski, L. M., & Gendelman, H. E. (2009). Neurodegenerative disorders and nano formulated drug development. Nanomedicine, 4(5), 541-555. https://doi.org/10.2217/nnm.09.37
23. Sagar, A., Karole, S., Chakraborty, A. K., &Loksh, K. R. (2022). Formulation, development, and characterization of topical organogel of mometasone furoate for the treatment of skin disease. *Indian Journal of Pharmacy and Pharmacology*. Retrieved from https://www.ijpp.org.in/
24. Hamidi, M., Azadi, A., &Rafiei, P. (2008). Hydrogel nanoparticles in drug delivery. Advanced Drug Delivery Reviews, 60(15), 1638-1649. https://doi.org/10.1016/j.addr.2008.08.002